

Complete the Planned FY 2024 Design Parameters Development at INL to Support the Drafting of the A709 Near-Term Code Case

INL/RPT-24-80602
Revision 0

Advanced Reactor Technologies

SEPTEMBER 2024

Heramb Mahajan

Idaho National Laboratory

Richard Wright

Subject Matter Expert



DISCLAIMER

This information was prepared as an account of work sponsored by an agency of the U.S. Government. Neither the U.S. Government nor any agency thereof, nor any of their employees, makes any warranty, expressed or implied, or assumes any legal liability or responsibility for the accuracy, completeness, or usefulness, of any information, apparatus, product, or process disclosed, or represents that its use would not infringe privately owned rights. References herein to any specific commercial product, process, or service by trade name, trade mark, manufacturer, or otherwise, does not necessarily constitute or imply its endorsement, recommendation, or favoring by the U.S. Government or any agency thereof. The views and opinions of authors expressed herein do not necessarily state or reflect those of the U.S. Government or any agency thereof.

Complete the Planned FY 2024 Design Parameters Development at INL to Support the Drafting of the A709 Near-Term Code Case

**Heramb Mahajan
Idaho National Laboratory
Richard Wright
Subject Matter Expert**

September 2024

**Idaho National Laboratory
Advanced Reactor Technologies
Idaho Falls, Idaho 83415**

<http://www.inl.gov>

**Prepared for the
U.S. Department of Energy
Office of Nuclear Energy
Under DOE Idaho Operations Office
Contract DE-AC07-05ID14517**

Page intentionally left blank

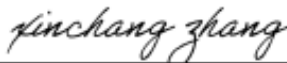
INL ART Program

**Complete the Planned FY 2024 Design Parameters
Development at INL to Support the Drafting of the
A709 Near-Term Code Case**

INL/RPT-24-80602
Revision 0

September 2024

Technical Reviewer: (Confirmation of mathematical accuracy, and correctness of data and appropriateness of assumptions.)




Xinchang Zhang
Materials Engineer

9/10/2024

Date

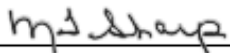
Approved by:



Michael E. Davenport
ART Project Manager

9/10/2024

Date



Michelle T. Sharp
INL Quality Assurance

9/10/2024

Date

SUMMARY

This report presents the thermophysical properties measurements conducted in the fiscal year 2024 to extend the material properties database up to 1000°C. The new values are compared against properties of high molybdenum steels in the American Society of Mechanical Engineers (ASME) Section II Part D tables. This report also shows the comparison between new measurements against the previously measured values in literature and provides recommended thermophysical properties for A709 code case. These values will support the thermophysical property tables in the near-term code case of A709.

Page intentionally left blank

ACKNOWLEDGEMENTS

This research was sponsored by the U.S. Department of Energy (DOE) under Contract No. DE-AC07-05ID14517 with Idaho National Laboratory (INL). Programmatic direction was provided by the Office of Nuclear Reactor Deployment of the DOE Office of Nuclear Energy (NE).

The authors gratefully acknowledge the support provided by Sue Lesica of DOE-NE, federal materials lead for the Advanced Reactor Technologies (ART) Program; Kaatrin Abbott of DOE-NE, federal manager, ART Fast Reactor Program (FRP); and Bo Feng of Argonne National Laboratory, national technical director, ART FRP. Authors gratefully acknowledge Ting-Leung Sham of the U.S. Nuclear Regulatory Commission, who served as the Advanced Materials Technology Area Lead for the ART Program within DOE-NE prior to joining the US-NRC, for his technical guidance.

The authors gratefully acknowledge Arin Preston, Robin Roper, Zilong Hua, Amey Khanolkar, and David Cottle, of INL for their testing support.

Page intentionally left blank

CONTENTS

SUMMARY	v
ACKNOWLEDGEMENTS	v
ACRONYMS	x
1. INTRODUCTION	1
2. MATERIAL	2
3. THERMOPHYSICAL PROPERTIES	2
3.1. Expansion coefficient	2
3.2. Specific Heat Capacity	4
3.3. Thermal Diffusivity	5
3.4. Thermal conductivity	6
3.5. Elastic Moduli and Poisson's Ratio	7
4. DISCUSSIONS	8
5. SUMMARY	10
6. REFERENCES	10

FIGURES

Figure 1. Comparison of linear expansion coefficient measurements with cubic fitting function against literature values and material properties in Group 4 Section II, Part D.	3
Figure 2. Mean and instantaneous expansion coefficient plots with respective fitting function and comparisons with literature values and Group 4 material properties in Section II, Part D.	4
Figure 3. Specific heat capacity measurements of new data and literature values and average specific heat values with extrapolated values beyond 850°C.	5
Figure 4. Comparison of thermal diffusivity with quadratic fitting function against the literature data and material properties under Group K, Section II, Part D.	6
Figure 5. Comparison of calculated thermal conductivity against reported values in literature and material properties under Group K, Section II, Part D.	7
Figure 6. Comparison of elastic moduli values in literature with a linear fitting function against material data under Group J, Section II, Part D.	8

TABLES

Table 1. Chemical composition of commercial heat of A709 used for new thermophysical property measurements in weight (%).	2
Table 2. Temperature dependent thermophysical properties of A709.	8

Page intentionally left blank

ACRONYMS

ART	Advanced Reactor Technologies
ASME	American Society of Mechanical Engineers
ASTM	American Society for Testing and Materials
BPVC	Boiler and Pressure Vessel Code
PT	Precipitation treatment
SA	Solution Annealing
SFR	Sodium-cooled Fast Reactor

Page intentionally left blank

Complete the Planned FY 2024 Design Parameters Development at INL to Support the Drafting of the A709 Near-Term Code Case

1. INTRODUCTION

Sodium-cooled fast reactor (SFR) deployment is a key step towards a zero-carbon emission goal. The SFR construction and deployment are dependent on the development of advanced materials. The goal of the materials development of the Fast Reactor Campaign of the Advanced Reactor Technologies (ART) program within the Office of Nuclear Energy of the U.S. Department of Energy is to develop and qualify advanced structural materials to enable improved reactor performance. Higher reactor efficiency is expected at elevated temperatures. Thus, materials with higher performance at elevated temperatures can reduce the SFR component construction costs, enabling the economic viability of SFRs and enable higher safety margins over longer operating times.

A709 is an austenitic stainless steel with a better performance characteristic at elevated temperatures than 316H stainless steel. A significant effort to optimize and evaluate the material properties by three laboratories—Argonne National Laboratory, Idaho National Laboratory, and Oak Ridge National Laboratory—led to the selection of A709 as a candidate material for American Society of Mechanical Engineers (ASME) Boiler and Pressure Vessel Code (BPVC), Section III, Division 5 [1]. This code provides component-construction rules operating in the creep regime under cyclic loads. To developing designed material properties, Section III, Division 5, requires material property data from a minimum of three commercial heats. A staged code-qualification plan and a test plan supporting the code case were developed [2].

Significant work was done to optimize heat treatment of A709, evaluate its mechanical properties, and develop a data package for A709 over last few years [3–11]. These studies explored the microstructure and mechanical properties and evaluated the influence of different heat treatments on microstructure and mechanical properties. The solution-annealing (SA) temperature of 1,150°C or higher yielded the best creep properties, but with creep-fatigue properties that were less than optimal. Plates in SA states have been characterized and documented in past reports [3,8,9]. Additional heat treatment of 775°C for 10 hours, referred as PT, achieved a balance in creep and creep-fatigue properties through the precipitation of beneficial Nb-rich nano precipitates [6,7,11]. A709 material with SA followed by PT condition, referred as A709-PT in this report, is selected to support the code case.

Using A709-PT material properties database, allowable stresses and design curves were determined. The development work is summarized in a report by Barua and Messner [12]. One of the requirements of the near-term code case involves thermophysical properties from room temperature to the maximum design temperature. Previous work has measured the thermophysical properties of A709 up to 850°C, and the experimentation has been published [13,14]. There is a need to measure and document the thermophysical properties up to 950°C to support the timely deployment of the near-term code case of A709-PT.

This report presents the thermophysical properties measurements conducted in fiscal year 2024. Thermophysical properties tabulated in Section II Part D of the ASME BPVC are grouped by alloy type. Values determined for A709 are compared against the high Molybdenum steels in the ASME Section II Part D tables [15]. This report also provides a comparison between new measurements and the previously measured values and offers recommended thermophysical properties for A709 code case.

2. MATERIAL

This report uses A709 plate product form from fabricator ATI Specialty Rolled Products with commercial heat number 529900. Argon-oxygen decarburization followed by electroslag remelting technique produced ingots. These ingots were hot rolled into plate form, which were SA at a minimum temperature of 1,150°C. All plates used for code-case testing were PT at 775°C for 10 hours in air and then were air cooled. Small samples were machined for thermophysical properties from plate using wire-electrical discharge machining. The nominal grain size of plate was ASTM grain number 7. The chemistry of this plate heat is listed in Table 1. ASME BPVC SA213/SA213M-23 specification [16] provides the chemistry specification for A709 seamless tubing form and is listed for reference in Table 1.

Table 1. Chemical composition of commercial heat of A709 used for new thermophysical property measurements in weight (%).

Fabricator	Heat #	C	Cr	Co	Ni	Mn	Mo	N	Si
ATI-1	529900	0.08	19.9	0.02	24.6	0.9	1.5	0.15	0.39
ASME SA-213		0.1 max	19.5– 23.0		23.0– 26.0	1.50 max	1.0–2.0	0.10– 0.25	1.00 max
Fabricator	Heat #	P	S	Ti	Nb	Al	B	Cu	Fe
ATI-1	529900	0.003	<0.001	< 0.01	0.17	0.02	0.004	0.06	Bal.
ASME SA-213		0.030 max	0.030 max	0.20 max	0.10– 0.40		0.002– 0.010		

3. THERMOPHYSICAL PROPERTIES

3.1. Expansion coefficient

A cylindrical sample measuring 12.5 mm in diameter and 25 mm length was machined from A709-PT plate and used for expansion coefficient measurement. Linear thermal expansion measurements (dL/L_0) were carried out using a Netzsch Model DIL 402 dilatometer. Measurements were performed according to American Society for Testing and Materials (ASTM) E228-11 at a heating rate of 3°C/minute. Data were recorded at 10°C increments. The plot in Figure 1 shows the comparison of linear thermal expansion as a function of temperatures. New data measured up to 1,000°C for this report are referred as fiscal year 2024. This data is compared against the previously measured data [13]. The Group 4 stainless steel data properties in ASME Section II, Part D, Table TE-1 Thermal Expansion of Ferrous Materials matched well with the measured data. A quadratic fitting function is used to fit the data up to 1,000°C, as shown in Figure 1, with corresponding coefficient of determination value. The fitting function for mean expansion coefficient, f_{lec} , is given in Equation (1).

$$\alpha_{linear} = 2.0217 \times 10^{-6} T^2 + 1.6804 \times 10^{-2} - 0.49678 \quad (1)$$

Where,

T = temperature in °C.

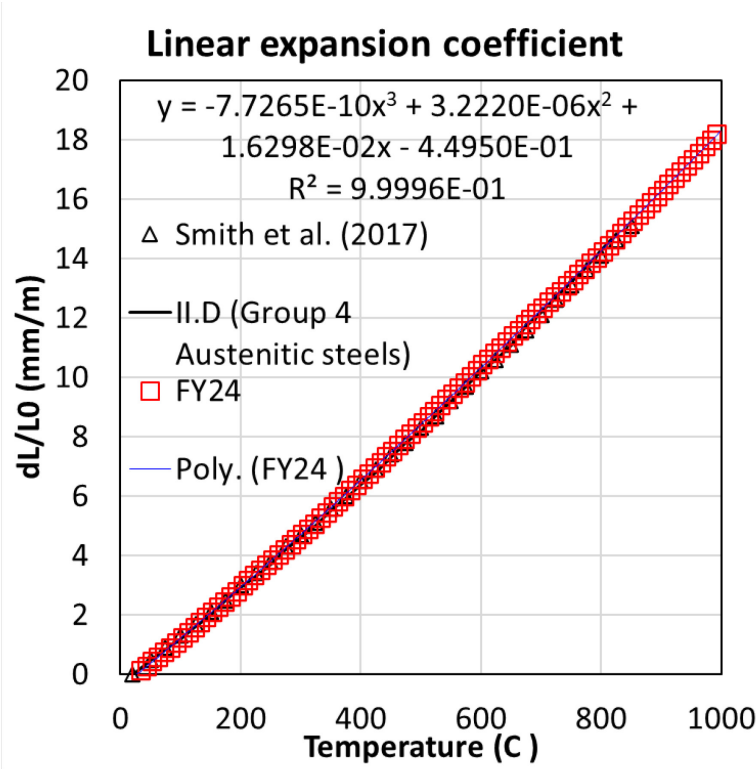


Figure 1. Comparison of linear expansion coefficient measurements with cubic fitting function against literature values and material properties in Group 4 Section II, Part D.

The mean expansion coefficient is calculated using Equation (2).

$$\alpha_{mean} = \frac{\left(\frac{dL}{L_0} \Big|_T - \frac{dL}{L_0} \Big|_{T_0} \right)}{(T - T_0)} \quad (2)$$

Where,

$\frac{dL}{L_0} \Big|_T$ = is linear expansion coefficient measured at target temperature

$\frac{dL}{L_0} \Big|_{T_0}$ = is linear expansion coefficient measured at room temperature

T_0 = room temperature

The plot on left side in Figure 2 shows the calculated mean expansion coefficient values. The calculated values match reasonably well with previously measured values and report values for NF709 [17]. The Group 4 stainless steel data properties in ASME Section II, Part D, Table TE-1 could be used as reference values for lower temperatures values. Instantaneous expansion coefficient is calculated as the first derivative with respect to the fitting function temperature of the linear expansion coefficient, as shown in Equation (3) and the right side of Figure 2. These values are compared against the previously measured data and Group 4 in Section II, Part D, Table TE-1. As error between measured values and extrapolated values from Section II, Part D were significant, fitting functions using measured data is recommended.

$$\alpha_{inst} = \alpha'_{linear}(T) \quad (3)$$

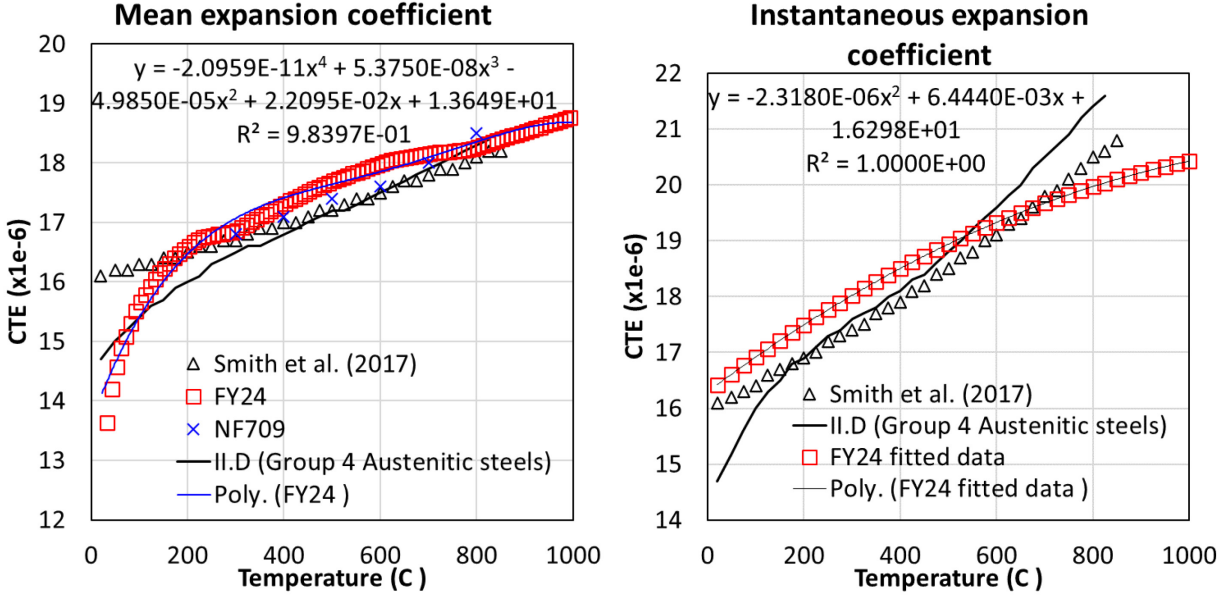


Figure 3. Mean and instantaneous expansion coefficient plots with respective fitting function and comparisons with literature values and Group 4 material properties in Section II, Part D.

3.2. Specific Heat Capacity

The specific heat capacity is required to calculate the thermal conductivity as discussed in 3.4 below. A disk sample, with a 4 mm diameter and 1 mm thickness, was machined from A709 plate for specific heat capacity measurements. Differential scanning calorimetry (DSC) was used with a heating rate of 10°C/minute. The sample was placed in glassy carbon crucible under an argon gas environment. Specific heat (C_p) at a given temperature is measured using a multi-phase process. First, a baseline is measured using an empty crucible subjected to the same temperature program as the test sample. Second, the heat capacity of a standard, such as sapphire, is measured with the same temperature program. Third, the heat capacity of the sample is measured. The heat capacity of the sample is calculated by using Equation (4).

$$C_p = \frac{m_{standard}}{m_{sample}} * \frac{DSC_{sample} - DSC_{baseline}}{DSC_{standard} - DSC_{baseline}} * C_{p,standard} \quad (4)$$

Where,

$C_{p,standard}$ = specific heat of the standard (e.g., sapphire) at temperature

m = mass

DSC = value of the DSC signal at temperature.

The measured specific heat values as a function of temperatures are presented in the left plot in Figure 3. Specific heat values increase monotonically up to 550°C. A sharper increase in specific heat values is observed in all new samples from 550 to 625°C compared to the previous measurements. Beyond 625°C, specific heat values showed a minimal increase with increasing temperature. Thus, values from 650–850°C were used to extrapolate data up to 1,000°C using linear fitting function, as shown in the right plot in Figure 3. Conductivity is calculated using average values up to 850°C and extrapolated values beyond 850°C using Equation (5).

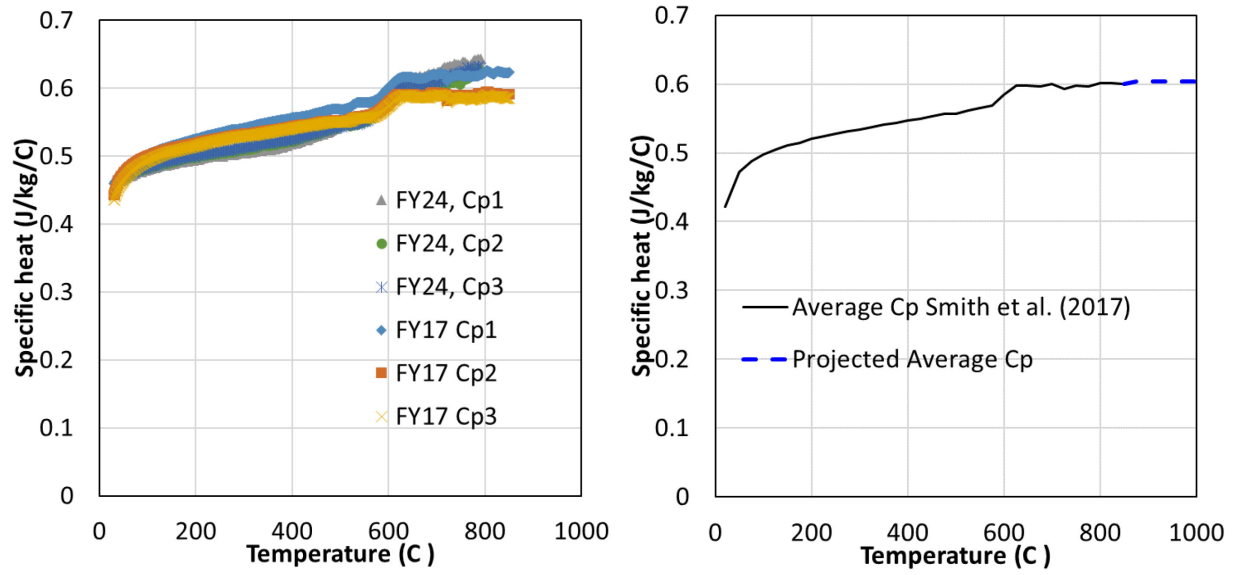


Figure 4. Specific heat capacity measurements of new sample data and reported values in literature values and average specific heat values with extrapolated values beyond 850°C.

$$C_p|_{T>850} = 0.5944 + 2.9764 \times 10^{-6}T \quad (5)$$

3.3. Thermal Diffusivity

A disk sample, with an 8 mm diameter and 2 mm thickness, was machined for thermal diffusivity measurements. New diffusivity measurements recorded up to 1,000°C are presented in Figure 4. Diffusivity values documented for Group K stainless steel material under ASME Section II, Part D, Table TCD are depicted in Figure 4 by solid black line. At lower temperatures, data points match very well with Group K values. Although some deviation is observed at higher temperatures between new measured values and Group K values, the general slope of line is consistent. The extrapolated Group K values using the linear fitting function is illustrated by a dashed blue line in Figure 4. The fitting function for new data is shown in solid line listed as Poly (FY 24) in Figure 4. Due to small deviation at higher temperature, error between measured values and the extrapolated Group K Section II Part D values was calculated. At 950°C, the calculated error between measured values and extrapolated values was 6.6% which is below 10%. Thus, the extrapolation of Group K, Section II, Part D, properties using linear equation highlighted in blue color shown in Figure 4 is recommended.

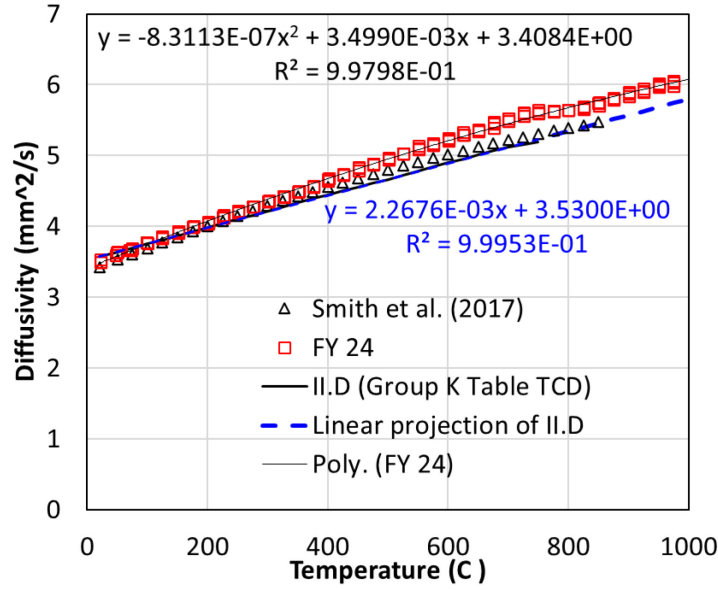


Figure 5. Comparison of thermal diffusivity with quadratic fitting function against the literature data and material properties under Group K, Section II, Part D.

3.4. Thermal conductivity

Thermal conductivity (κ) is calculated using Equation (6).

$$\kappa = D\rho_T C_p \quad (6)$$

Where,

D = thermal diffusivity in (m^2/s)

ρ_T = temperature specific density (kg/m^3)

C_p = specific heat (J/kgK).

For density measurement, a disk sample with an 8 mm diameter and 2 mm thickness, was machined from ATI-1-PT heat #529900. The sample weight was measured dry, then boiled in water for 20 minutes per the ASTM standard. The submerged and wet masses were recorded. Four measurements were taken for each step and were averaged them, then performed the density calculations. Based on the measurements a density calculation was made. The sample was selected as a zero-porosity medium. The room temperature density was 7.90368 g/cm^3 . Linear expansion coefficient measurements, $\frac{dL}{L_0}$, documented in the previous subsection were used to calculate the temperature specific density, ρ_T , using Equation (7).

$$\rho_T = \frac{\rho_0}{\left(1 + \frac{dL}{L_0}\right)^3} \quad (7)$$

Where,

ρ_0 = density at room temperature.

Using temperature corrected specific density, a thermal conductivity is calculated. The extrapolated diffusivity values using linear fitting function from Section II Part D table is used. Figure 5 presents the calculated conductivity against previous data [13] and ASME Section II, Part D, Group K material. An agreement is observed between all values until 600°C. As shown in the previous two subsections, from 600–700°C, nonlinear behavior is observed in diffusivity and specific heat measurements. Although this nonlinear behavior results in small deviation in conductivity measurements, extrapolated Group K, Section II, Part D values using the linear fitting function highlighted in blue color in Figure 5, captures the general trend of calculated values. The absolute percent error between calculated values and extrapolated values from Section II Part D values at 950°C is 8.99% which is smaller than 10%. Thus, for conductivity measurements using Group K values with linear extrapolation is recommended.

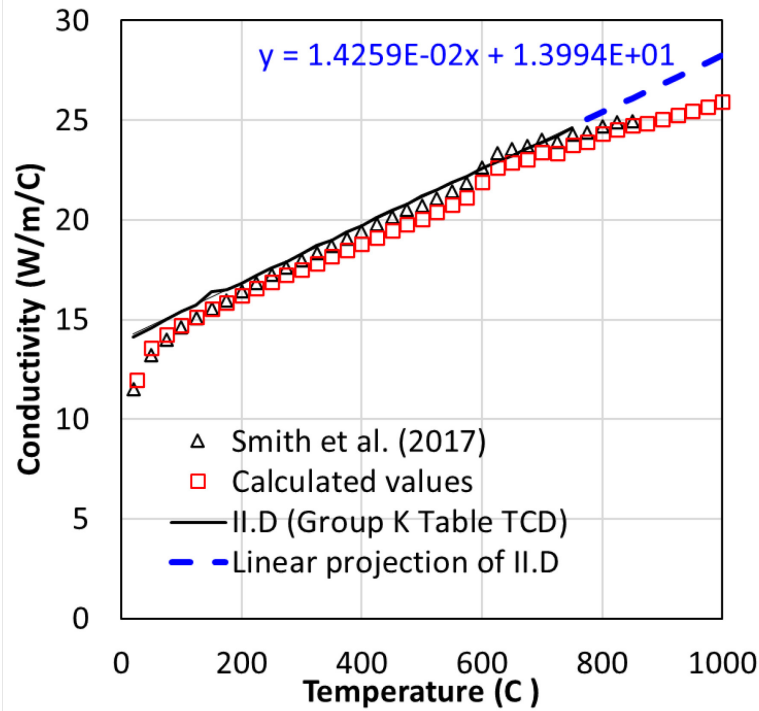


Figure 6. Comparison of calculated thermal conductivity against reported values in literature and material properties under Group K, Section II, Part D.

3.5. Elastic Moduli and Poisson's Ratio

A disk sample with an 8 mm diameter and 2 mm thickness was machined for modulus measurements. A laser ultrasound technique was used to measure elastic moduli and Poisson's ratio [14]. The data reported in the previous work [14] is compared against the Group J, Section II, Part D material values and reported elastic moduli for the NF709 reported in the Nippon Steel vendor data sheet. All these values compare well against each other. The recorded values show a good linear trend from room temperature up to 850°C. Additional experimental values for higher temperatures were not obtained in FY 24. Thus, extrapolation of elastic moduli values is suggested up to 950°C with a linear fitting function highlighted in blue color as shown in Figure 6. The laser ultrasound technique also provided a temperature dependent Poisson's ratio. The previously documented extrapolation function [14] is used to determine the Poisson's ratio values, as presented in Equation (8).

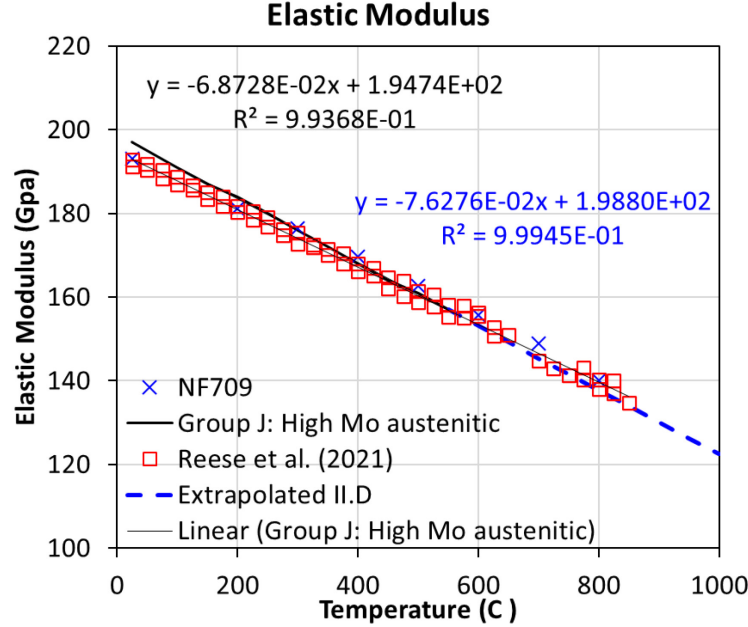


Figure 7. Comparison of elastic moduli values in literature with a linear fitting function against material data under Group J, Section II, Part D.

$$\nu = 0.28 + 6.6527 \times 10^{-5}T \quad (8)$$

4. DISCUSSIONS

Table 2 lists the recommended thermophysical properties of A709 either using the extrapolated Section II, Part D properties or using fitting function based on measured data. Linear fitting function using Section II Part D properties is recommended for elastic modulus (E). Linear fitting functions was used for Poisson's ratio (ν) using measured data to interpolate values up to 850°C and extrapolate beyond 850°C. A cubic fitting function was used to fit linear expansion coefficient values α_{linear} . This cubic equation was used to list tabulated values. Instantaneous (α_{inst}) and mean (α_{mean}) expansion coefficient values were tabulated using a quadratic and a fourth order polynomial function, respectively. Section II, Part D diffusivity values up to 750°C was used to fit linear function and this function is used to extrapolate diffusivity values up to 950°C. Documented values of heat capacity in “Thermophysical properties of Alloy 709” [13] were used as is without any fitting function up to 850°C. Linear fitting function extrapolated these values up to 950°C. Temperature-dependent density values were calculated from room temperature density and linear expansion coefficient values. Conductivity is calculated using diffusivity, heat capacity, and density. The shaded cells in Table 2 show calculated or extrapolated values using fitting equations.

Table 2. Recommended temperature dependent thermophysical properties of A709.

T (°C)	E (MPa)	ν	α_{inst} ($\times 10^{-6}$ mm/mm)	α_{mean} ($\times 10^{-6}$ mm/mm)	α_{linear} (mm/m)	D (mm ² /s)	ρ_T (g/cc)	C_p (J/(g*K))	κ (W/m°C)
25	197	0.279	16.9	14.2	-0.0754	3.59	7.91	0.422	12
50	195	0.281	17	14.6	0.348	3.64	7.9	0.472	13.6
75	193	0.282	17.1	15	0.775	3.7	7.89	0.488	14.2
100	191	0.284	17.2	15.4	1.2	3.76	7.88	0.498	14.7

T (°C)	E (MPa)	ν	α_{inst} ($\times 10^{-6}$ mm/mm)	α_{mean} ($\times 10^{-6}$ mm/mm)	α_{linear} (mm/m)	D (mm ² /s)	ρ_T (g/cc)	C_p (J/(g*K))	κ (W/m°C)
125	189	0.286	17.3	15.7	1.64	3.81	7.87	0.505	15.1
150	187	0.288	17.4	16	2.07	3.87	7.85	0.511	15.5
175	185	0.289	17.5	16.3	2.51	3.93	7.84	0.515	15.9
200	184	0.291	17.6	16.5	2.94	3.98	7.83	0.52	16.2
225	182	0.293	17.7	16.7	3.39	4.04	7.82	0.524	16.6
250	180	0.295	17.8	16.8	3.83	4.1	7.81	0.528	16.9
275	178	0.297	17.9	17	4.28	4.15	7.8	0.532	17.2
300	176	0.298	18	17.1	4.73	4.21	7.79	0.534	17.5
325	174	0.3	18.1	17.2	5.18	4.27	7.78	0.537	17.8
350	172	0.302	18.2	17.3	5.63	4.32	7.77	0.541	18.2
375	170	0.304	18.3	17.3	6.09	4.38	7.76	0.544	18.5
400	168	0.305	18.4	17.4	6.55	4.44	7.75	0.547	18.8
425	166	0.307	18.5	17.5	7.01	4.49	7.74	0.55	19.1
450	164	0.309	18.6	17.5	7.47	4.55	7.73	0.553	19.4
475	163	0.311	18.7	17.6	7.94	4.61	7.72	0.557	19.8
500	161	0.312	18.8	17.6	8.41	4.66	7.71	0.557	20
525	159	0.314	18.9	17.7	8.88	4.72	7.7	0.561	20.4
550	157	0.316	19	17.7	9.36	4.78	7.69	0.565	20.7
575	155	0.318	19.1	17.8	9.83	4.83	7.68	0.569	21.1
600	153	0.319	19.2	17.9	10.3	4.89	7.66	0.584	21.9
625	151	0.321	19.3	17.9	10.8	4.95	7.65	0.598	22.6
650	149	0.323	19.4	18	11.3	5	7.64	0.598	22.9
675	147	0.325	19.5	18	11.8	5.06	7.63	0.597	23.1
700	145	0.327	19.6	18.1	12.3	5.12	7.62	0.6	23.4
725	143	0.328	19.7	18.2	12.7	5.17	7.61	0.593	23.3
750	142	0.33	19.8	18.2	13.2	5.23	7.6	0.598	23.8
775	140	0.332	19.9	18.3	13.7	5.29	7.59	0.596	23.9
800	138	0.334	20	18.4	14.2	5.34	7.58	0.601	24.3
825	136	0.335	20.1	18.4	14.7	5.4	7.56	0.601	24.6
850	134	0.337	20.2	18.5	15.2	5.46	7.55	0.6	24.7
875	132	0.339	20.3	18.5	15.8	5.51	7.54	0.597	24.8
900	130	0.341	20.4	18.6	16.3	5.57	7.53	0.597	25
925	128	0.342	20.5	18.6	16.8	5.63	7.52	0.597	25.3
950	126	0.344	20.6	18.7	17.3	5.68	7.51	0.597	25.5

5. SUMMARY

This report summarizes the thermophysical data recorded to develop material properties of A709. These values are compared against the previously documented values and show a good correlation. Appropriate properties from ASME Section II, Part D, tables are compared against data and show a good comparison at lower temperature range. Fitting functions are presented in respective plots, and these functions are used to present the data with 25°C temperature increments. Diffusivity, expansion coefficient, and density values were measured and reported up to 1,000°C. Fitting functions were used to extrapolate data beyond 850°C for moduli, Poisson's ratio, and specific heat measurements.

6. REFERENCES

1. ASME. 2023. "BPVC Section III Rules for Construction of Nuclear Facility Components-Division 5-High Temperature Reactors." American Society of Mechanical Engineers. BPVC-III.5.
2. Sham T.-L., and K. Natesan. 2017. "Code Qualification Plan for an Advanced Austenitic Stainless Steel, Alloy 709, for Sodium Fast Reactor Structural Applications." International Conference on Fast Reactors and Related Fuel Cycles: Next Generation Nuclear for Sustainable Development (FR17), IAEA-CN-245-74.
3. McMurtrey, M. D., and R. E. Rupp. 2019. "Report on FY19 Scoping Creep and Creep-Fatigue Testing on Heat Treated Alloy 709 Base Metal." INL/EXT-19-55502-Rev000. Idaho National Laboratory, Idaho Falls, ID. <https://www.osti.gov/biblio/1847949>.
4. Rupp, R. E., and M. D. McMurtrey. 2020. "Status of INL Aged A709 Mechanical Testing." INL/EXT-20-59501-Rev000. Idaho National Laboratory, Idaho Falls, ID. <https://www.osti.gov/biblio/1688795>.
5. Sham, T. -L., R. E. Bass, Y. Wang, and X. Zhang. 2022. "A709 Qualification Plan Update and Mechanical Properties Data Assessment." INL/RPT-22-67641-Rev000. Idaho National Laboratory, Idaho Falls, ID. <https://www.osti.gov/biblio/1906516>.
6. Mohale, N., and R. E. Bass. 2022. "Microstructural Characterization of A709 Commercial Heats with Precipitation Treatment." INL/RPT-22-68666-Rev000. Idaho National Laboratory, Idaho Falls, ID. <https://www.osti.gov/biblio/1906443>.
7. Bass, R. E., and T. -L. Sham. 2022. "Interim Creep, Fatigue and Creep-Fatigue Data from FY 2022 INL Testing of A709 with Precipitation Treatment for ASME Code Case Data Package." INL/RPT-22-68982-Rev000. Idaho National Laboratory, Idaho Falls, ID. <https://www.osti.gov/biblio/1906448>.
8. Bass, R. E., and T. -L. Sham. 2022. "Initial Characterization of the Second A709 Commercial Heat." INL/RPT-22-69073-Rev000. Idaho National Laboratory, Idaho Falls, ID. <https://www.osti.gov/biblio/1906451>.
9. Patterson, T., Y. Wang, and T. -L. Sham. 2023. "A Summary of the Microstructural Characterization Results for the A709 Commercial Heats." INL/RPT-23-74406-Rev000. Idaho National Laboratory, Idaho Falls, ID. <https://www.osti.gov/biblio/1998572>.
10. Mahajan, H. P., et al. 2023. "A Summary of the Mechanical Properties Data Developed in FY 2023 by ANL, INL, and ORNL to Support the Data Package Development for the A709 Code Case." INL/RPT-23-74680-Rev000. Idaho National Laboratory, Idaho Falls, ID. <https://www.osti.gov/biblio/2008356>.
11. Zhang, X. 2023. "Microstructural Investigation of Precipitation Treated A709 Test Samples." ANL-ART-272. Argonne National Laboratory, Lemont, IL. <https://doi.org/10.2172/2001067>.
12. Barua, B., and M. C. Messner. 2024. "ASME Section III, Division 5, Class A 100,000-Hour Design Data for Alloy 709." ANL-ART-285, Argonne National Laboratory, Lemont, IL.

13. Smith, D. S., N. J. Lybeck, J. K. Wright, and R. N. Wright. 2017. "Thermophysical Properties of Alloy 709." *Nuclear Engineering and Design* 322: 331–335.
14. Reese, S. J., et al. 2021. "Elevated-Temperature Elastic Properties of Alloys 709 and 617 Measured by Laser Ultrasound." *Journal of Materials Engineering and Performance* 30: 1513–1520.
<https://doi.org/10.1007/s11665-020-05430-4>.
15. ASME. 2023. "BPVC Section II Materials Part D Properties." American Society of Mechanical Engineers. BPVC-II.D.
16. ASTM International. 2023. "Standard Specification for Seamless Ferritic and Austenitic Alloy-Steel Boiler, Superheater, and Heat-Exchanger Tubes." ASTM A213/A213M-23.
17. NF709 Material Data Sheet. 2013. Nippon Steel and Sumitomo Metal Corporation, Tokyo, Japan. April 11, 2013.